ISSN 1995-0780, Nanotechnologies in Russia, 2020, Vol. 15, Nos. 11–12, pp. 747–752. © Pleiades Publishing, Ltd., 2020.
Russian Text © The Author(s), 2020, published in Rossiiskie Nanotekhnologii, 2020, Vol. 15, No. 6, pp. 781–786.

FUNCTIONAL AND CONSTRUCTION NANOMATERIALS

Formation of Nanoporous Films during Solid-Phase Reactions

A. V. Butashin[a], **A. E. Muslimov**[a,*], **A. Sh. Asvarov**[a,b], **and V. M. Kanevsky**[a]

[a] *Shubnikov Institute of Crystallography, Federal Scientific Research Center "Crystallography and Photonics," Russian Academy of Sciences, Moscow, 119333 Russia*

[b] *Amirkhanov Institute of Physics, Dagestan Federal Research Center, Russian Academy of Sciences, Makhachkala, 367015 Russia*

**e-mail: amuslimov@mail.ru*

Received August 31, 2020; revised October 1, 2020; accepted October 1, 2020

Abstract—Specific features of the formation of nanoporous Al_2O_3, AlN, and $Ni(Fe+Al)_2O_4$ films on sapphire substrates by thermal sputtering of metals with subsequent firings in an appropriate gas medium are studied. This synthesis process involves interaction of the metal solid phase with an active ambient gas medium (oxygen or nitrogen), some other chemical reactions, diffusion, and crystallization. It can be controlled via a set of synthesis parameters to achieve desired film properties and structure. It is shown that variations in the thickness of initial metal films, annealing temperature and time, and sample heating rate affect the run and completeness of the above processes and allow one to obtain films with a required structure (in particular, films with a nanoporous structure with pores 10–200 nm in size).

DOI: 10.1134/S1995078020060051

INTRODUCTION

Nanoporous films and coatings are of great interest for researchers and engineers, due to their properties caused by violation of homogeneity of the solid phase. The most important representatives are "porous silicon," with its unique optical properties [1], cellular layers of anodized aluminum [1], various porous metal and oxide structures [2], and polymer track membranes [3] as a basis for the technology of template synthesis of micro- and nanostructures. A surface of sapphire substrates with a microrelief for epitaxy of single-crystal AlN and GaN films at significant mismatch between substrate and film metrics can also be considered as a porous coating [4]. Chemical and electrochemical etching, in combination with ionizing irradiation or photolithography, are widely applied for the formation of porous films and coatings [1, 3, 4]. The range of application of continuous thin films of various compositions in micro- and optoelectronics, electrical engineering, informatics, and sensorics continuously increases, as well; methods of formation of functional thin films with desired composition and structure have been developed [5].

Apparently, one of the simplest such methods implies thermal sputtering of metal onto a substrate and subsequent annealing in an appropriate gas medium: for example, polycrystalline films of the ZnO [2], Fe_2O_3 [6], and Al_2O_3 [7] compounds can be obtained using chemical reactions in the solid phase. Obviously, the processes of synthesis of polycrystalline or amorphous films by this way can be described and interpreted using methods of thermochemistry of metal and alloy surfaces [8].

In this paper, we report the results of studying specific features of the formation of nanoporous Al_2O_3, AlN, and $Ni(Fe+Al)_2O_4$ films on sapphire substrates by thermal sputtering of metals with subsequent firings in an appropriate gas medium. This synthesis process suggests interaction between the solid metal phase and air oxygen and significant inhomogeneity in the film structure and composition, which are determined by the type and rate of chemical reactions, diffusion, and crystallization. Variations in the thickness of initial metal films, annealing temperature and time, and sample heating rate affect the run and completeness of these processes and allow one to obtain films with a required structure (in particular, films with pores 10–200 nm in size).

EXPERIMENTAL

Experiments on the formation of aluminum thin films and their subsequent nitridation on (0001) sapphire substrates (Al/Al_2O_3) were carried out in a single vacuum cycle in a vacuum chamber with oilless pumping ($P_{res} \approx 2 \times 10^{-4}$ Pa) equipped with two independent resistive platinum heaters for the sputtered metal and substrate and observation windows. After placing a substrate and special-purity aluminum particles (99.999%) on corresponding heaters, the chamber was evacuated, and a metal layer 10–50 nm thick was deposited on the unheated substrate by thermal sput-

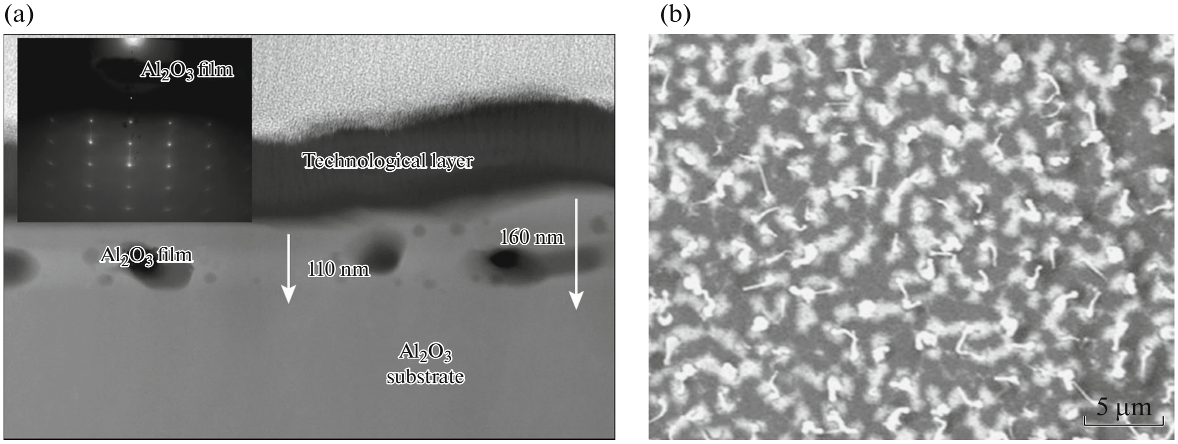

Fig. 1. (a) TEM image of the sapphire substrate with the nanoporous aluminum oxide film after annealing of the Al/Al_2O_3 composite in air at 1400°C for 1 h at a heating rate of ~300°C/h (the electron diffraction pattern from the film surface recorded in reflection geometry is given in the inset). (b) SEM image of the AlN/Al_2O_3 film surface heated to a temperature of 1200°C at a rate of ~300°C/h and kept for 1 h.

tering. Then the chamber was filled with special-purity nitrogen (using a GChA-18-KD nitrogen generator), and the substrate with the aluminum layer was heated to a temperature of 1200°C at different rates.

For oxidation experiments, Al films and multilayer structures containing Fe, Al, and Ni layers were deposited by the magnetron sputtering method. The magnetron sputtering setup was equipped with a turbomolecular pump providing limiting residual pressure of no higher than 1×10^{-3} Pa and three planar magnetron units for target sputtering. Metal (Al, Fe, and Ni) targets (purity 99.99%) were sputtered in 99.999%-pure argon at the operating pressure of 0.5 Pa in the discharge power stabilization mode (110 W). The substrates were original plates ~$10 \times 10 \times 0.5$ mm in size cut from standard sapphire substrates for epitaxy with the *C*(0001) orientation. The metal deposition rate and mean layer thickness were measured by a KIT 5 quartz meter. Subsequent annealing of the metal films in air was performed in the temperature range of 550–1400°C for 20–60 min using a tube furnace (Nabertherm).

The phase, chemical, and morphological analyses of the films obtained were carried out by X-ray diffraction methods on an X'PERT PRO diffractometer (PANalytical, the Netherlands) in the Bragg–Brentano reflection geometry using the CuK_α radiation ($\lambda = 1/5418$ Å) and a Ni β filter, transmission electron microscopy (TEM) using a Scios electron microscope, scanning electron microscopy (SEM) on a JEOL electron microscope, and energy-dispersive X-ray analysis (EDXA). Microhardness of the aluminum oxide films on sapphire were determined using a NanoSkan-3D scanning nanoindenter (TISNUM, Troitsk). Magnetization was measured with a Lake Shore vibrational magnetometer (model 7407) in fields up to 15 kOe at room temperature.

RESULTS AND DISCUSSION

Studies of the morphology of AlN and Al_2O_3 films grown on sapphire by solid-phase epitaxy showed that continuous films without pores are formed upon slow heating (50°C/h) of a metal film in an appropriate gas medium (N_2 or air) [9, 10]. Under the conditions of relatively fast heating of a furnace with a sample (≥300°C/h) to the solid-phase synthesis temperature, both closed and open porosity are formed in epitaxial structures of aluminum nitride and oxide. Figure 1a presents a cross-cut TEM image of the epitaxial Al_2O_3 film ~110–160 nm thick formed upon fast heating (300°C/h) of an aluminum thin film on sapphire in air

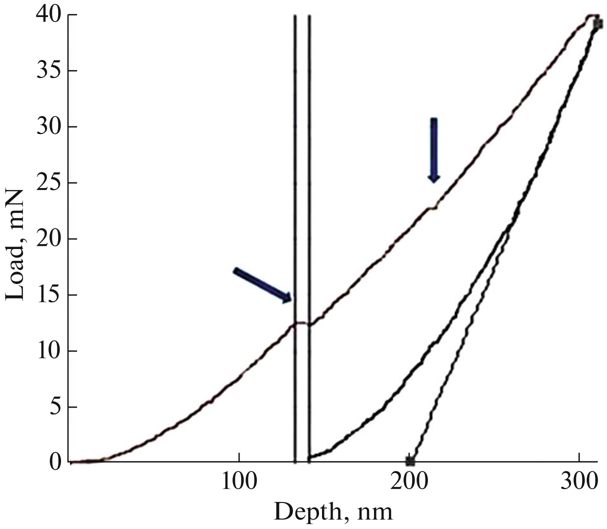

Fig. 2. Mechanical loading–unloading curves of the obtained nanoporous aluminum oxide films on sapphire. Arrows indicate steps due to the pop-in effect.

to a temperature of 1400°C and subsequent annealing at this temperature for 1 h. One can see that the formed oxide film contains pores with linear sizes up to 200 nm. The surface structure of the epitaxial AlN film obtained upon fast heating of the composite (Al/Al_2O_3) to a temperature of 1200°C in ultrapure nitrogen also indicates the porosity of its structure (Fig. 1b).

In addition, the mechanical properties of nanoporous aluminum oxide films grown on sapphire by solid-phase epitaxy were analyzed by recording loading–unloading curves (Fig. 2). A distinctive feature of the curves was the presence of pop-in effects [11, 12]. The first pop-in step, the length (8–18 nm) and position (120–150 nm) of which depend on the region of recording the curve in the sample, and the second step with a smaller length (5–8 nm) were found. The change in the position of the first pop-in step in the loading curves corresponds to a significant inhomogeneous in thickness of the Al_2O_3 film on sapphire (Fig. 1a) and indicates the local film–substrate interface. Different lengths of the first pop-in step in the curves indicate different thicknesses of the defect transition layer at the film–substrate interface, in which the whole plastic deformation is most likely concentrated. In addition, the curve slope changes significantly when passing from the film to the sapphire substrate, which indicates lower mechanical hardness of the porous film. The pop-in step observed upon deepening beyond 220 nm is related to achievement of the maximum shear stress under an indenter, which causes onset of plastic deformation in the sapphire substrate via nucleation of intragranular dislocations after the initial elastic portion in the curve. Note that the angle between the unloading curve and the abscissa axis is close to 50°–60°, which is indicative of pronounced elastic deformations in the sapphire bulk.

A ferrite spinel $Ni(Fe+Al)_2O_4$ film was synthesized using a more complex multilayer precursor, in which the bottom Fe layer and the top Ni layer were separated by a thin Al interlayer (Fig. 3). Annealing of the precursor in air at 750°C for 5 h led to oxidation of the components and formation of the $Ni(Fe+Al)_2O_4$ compound with a spinel structure and alloyed nickel and iron oxides (NiO:Fe, FeO:Ni, and Fe_2O_3:Ni). The X-ray diffraction pattern (Fig. 4) shows dominant content of the ferrite phase with a spinel structure in the synthesized film. It was difficult to estimate more thoroughly the phase composition, because of significant fluorescence observed in the X-ray diffraction pattern (Fig. 4), which was due to strong absorption of primary X-ray CuK_α radiation by the film material [13]. The formation of a film based on nickel ferrite spinel is also indicated by its ferromagnetic properties (Fig. 5). However, values of the saturation magnetization and coercive field for the obtained $Ni(Fe+Al)_2O_4$ film were much larger than those obtained previously for $NiFe_2O_4$ films [14], which indicates the presence of a significant fraction of the Fe_3O_4 magnetite phase in the synthesized film. In addition, the film is characterized by the absence of pronounced magnetic anisotropy inherent in epitaxial $NiFe_2O_4$ films.

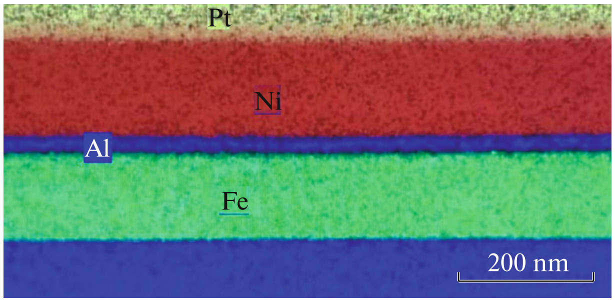

Fig. 3. (Color online) EDXA distribution map of Al, Ni, and Fe in the initial Ni/Al/Fe/sapphire multilayer structure.

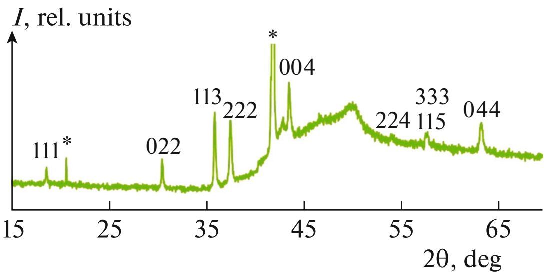

Fig. 4. (Color online) X-ray diffraction pattern of the Al–Ni–Fe/sapphire composite subjected to annealing in air at 750°C for 5 h: (indices) reflections of ferrite with a spinel structure, (*) substrate reflections, and (*I*) intensity.

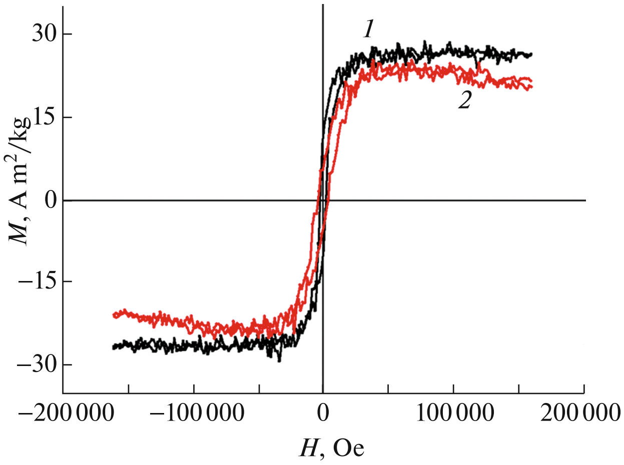

Fig. 5. (Color online) Magnetization curves of the ferrite spinel $Ni(Fe+Al)_2O_4$ film measured in a magnetic field applied (*1*) parallel and (*2*) perpendicular to the film plane.

Electron microscopy of cross cuts of the obtained nickel ferrite spinel film (Fig. 6) shows that its struc-

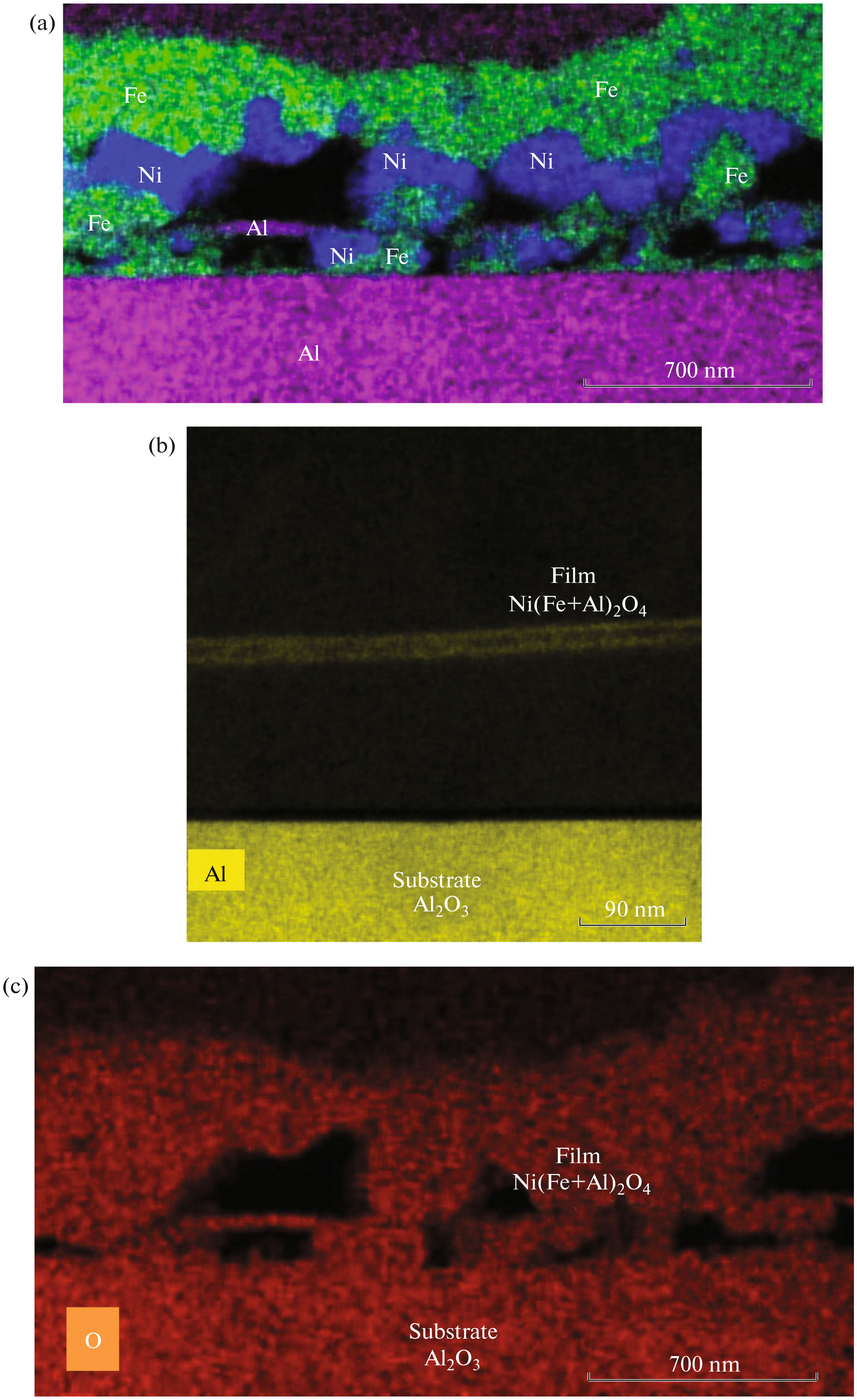

Fig. 6. (Color online) EDXA distribution maps of (a) Al, Ni, and Fe; (b) aluminum; (c) and oxygen in the Al–Ni–Fe/sapphire composite annealed in air at 750°C for 5 h.

ture differs significantly from that of $NiFe_2O_4$ films prepared from multilayer metal precursors with layer thicknesses from 1 to 2 nm [14]. Noteworthy features of Fig. 6a are displacement of significant iron amounts from the substrate above nickel layers, formation of large voids, and presence of an aluminum layer (obviously, in the form of oxide) at the same distance from the substrate (Fig. 6b) as in the initial precursor (Fig. 3). Complete oxidation of the multilayer precursor is also of interest (Fig. 6c).

A comparison of the structures of all films of three different compositions revealed the main factors that provide formation of nanoporous films. The observed formation of nanopores in the oxide or nitride films (Fig. 1) at these methods of their synthesis from a primary metal (aluminum) film can be due to the lag between the aluminum oxidation or nitridation processes and the processes of metal melting and evaporation in a space between the sapphire substrate and the strong oxide (or nitride) film on the metal surface, as well as the significant decrease in the metal density (down to 11%) in the liquid phase. The pressure on the still thin oxide (or nitride) film leads to the formation of hillocks on its surface and even its rupture. In this case, the governing parameters are thickness of the primary aluminum film (more than 50 nm) and high precursor heating rate during the synthesis of aluminum oxide or nitride films (~300°C/h or higher).

The observed structural features of the obtained film based on nickel ferrite spinel can be explained by significant differences in the activities of initial metals (Ni, Fe, and Al), the degrees of their oxygen affinity, which increases in the Ni–Fe–Al series, and the densities of metallic iron and iron oxides [14]. Indeed, air oxygen begins to diffuse intensely into the multilayer metal film upon heating of the precursor, and aluminum (the most active element) is first to be oxidized, forming a thin and strong aluminum oxide layer. Then the lower layer of rather active iron begins to be oxidized according to the reaction [15]

$$4Fe + 3O_2 = 2Fe_2O_3.$$

The density of oxide Fe_2O_3 is 33% lower than the metallic iron density; therefore, the layer of oxidized iron begins to expand in the normal and tangential (with respect to the substrate) directions. Mechanical coupling between the precursor layers due to diffusion of elements, chemical bonds, and tangential stress leads to the formation of discontinuities in aluminum and nickel oxide films, thus opening a channel for intense oxidation of metallic iron by air oxygen, while normal stress (pressure) carries away a significant amount of iron oxide to the film surface through these discontinuities. Voids inside a film based on nickel ferrite spinel can thus be formed. In this case, the governing parameters are thickness of primary metal (nickel and iron) layers (~200 nm), sequence of their deposition relative to the substrate, and the precursor heating rate upon annealing (~300°C/h or more).

CONCLUSIONS

It was shown by the example of Al_2O_3, AlN, and $Ni(Fe+Al)_2O_4$ films that nanoporous films can be formed without chemical etching by deposition on sapphire substrates by thermal sputtering of metals with subsequent annealing in an appropriate gas medium (due to the self-organization processes in materials upon annealing). The governing parameters for this synthesis process are the thicknesses of primary metal layers (~200 nm for nickel and iron and more than 50 nm for aluminum), the sequence of layer deposition relative to the substrate, and the precursor heating rate during annealing (~300°C/h or higher). We suggest that this approach can be implemented for the formation of nanoporous films with different compositions and unique optical and magnetic characteristics.

ACKNOWLEDGMENTS

We are grateful to N.S. Perov and Yu.V. Grigor’ev for their help in carrying out the experiments.

This study was performed on the equipment of the Shared Research Center “Structural Diagnostics of Materials” of the Shubnikov Institute of Crystallography of the Russian Academy of Sciences.

FUNDING

This study was supported by the Ministry of Science and Higher Education of the Russian Federation within a State assignment for the Federal Scientific Research Centre “Crystallography and Photonics” of the Russian Academy of Sciences in the part concerning “analysis of the processes of pore formation during synthesis of Al_2O_3 and AlN films” and the Russian Foundation for Basic Research, project nos. 18-02-00515 and 20-02-00373, in the part concerning “synthesis and characterization of films based on nickel ferrite and analysis of the processes of pore formation during synthesis.”

REFERENCES

1. Electrochemically Engineered Nanoporous Materials, Ed. by D. Losic and A. Santos, Vol. 220 of Springer Series in Material Science (Springer, Switzerland, 2015).
2. A. S. Asvarov, A. K. Abduev, A. K. Akhmedov, et al., Crystallogr. Rep. **63**, 994 (2018). https://doi.org/10.1134/S1063774518060032
3. B. V. Mchedlishvili, V. E. Asadchikov, A. I. Vilenskii, A. B. Vasil’ev, D. L. Zagorski, A. N. Nechaev,

V. A. Olenikov, A. V. Sergeev, V. N. Popok, N. D. Samotolin, and N. N. Mel'nik, Crystallogr. Rep. **48**, 140 (2003).

4. Y.-Kh. Ee, X.-H. Li, J. Biser, et al., J. Cryst. Growth **312**, 1311 (2010).
5. *Handbook of Crystal Growth. Thin Films and Epitaxy: Basic Techniques,* Ed. by Th. F. Kuech (Elsevier, UK, 2015), Vol. 3, part A.
6. M. Saleem, M. F. Al-Kuhaili, S. M. A. Durrani, and I. A. Bakhtiari, Phys. Scr. **85**, 055802 (2012).
7. L. P. H. Jeurgens, W. G. Sloof, F. D. Tichelaar, and E. J. Mittemeijer, J. Appl. Phys. **92**, 1649 (2002).
8. P. Kofstad, *High Temperature Oxidation of Metals* (Wiley, New York, 1966).
9. A. V. Butashin, A. E. Muslimov, A. L. Vasil'ev, et al., Prikl. Fiz., No. 6, 77 (2016).
10. A. V. Butashin, A. E. Muslimov, A. B. Kolymagin, et al., Prikl. Fiz., No. 5, 87 (2017).
11. G. M. Pharr, W. C. Oliver, and D. R. Clarke, J. Electron Mater. **19**, 881 (1990).
12. Sh. Chen, L. Liu, and T. Wang, Acta Mater. **52**, 1089 (2004).
13. Y. M. Mos, A. C. Vermeulen, C. J. N. Buisman, and J. Weijma, Geomicrobiol. J. **35**, 511 (2018).
14. V. M. Kanevsky, A. V. Butashin, and A. E. Muslimov, J. Surf. Invest.: X-ray, Synchrotron Neutron Tech. **12**, 1155 (2018).
15. V. I. Spitsin and L. I. Martynenko, *Inorganic Chemistry* (Mosk. Gos. Univ., Moscow, 1994), part 2 [in Russian].

Translated by A. Sin'kov